



Seismotectonic and Probabilistic Seismic Hazard of Sunda Strait Region

Asdani Soehaimi¹, Franto Novico¹, Mohammad Ridwan¹, Marina Claudia Frederik¹ and Suharsono¹

¹Research Center for Geological Disaster, National Research and Innovation Agency, Bandung, 40135, Indonesia

5

Correspondence to: Asdani Soehaimi (s.asdani@yahoo.com) and Franto Novico (franto12@yahoo.com)

Abstract. The Sunda Strait region is the riskiest area between Java and Sumatra. The impact of seismic activities must be considered to reduce disaster risk. This study has answered the lack of information about detailed seismotectonic conditions in the Sunda Strait. It confirms geotectonic actions controlled by the Asymmetry Subduction of the Sunda Arc between Oblique Subduction (Sumatra) and Frontal Subduction (Java). These activities produce five main seismotectonic zones based on their respective sources: Megathrust Seismotectonic Zones, Benioff Wadati Seismotectonic Zones, Sumatra Active Fault Seismotectonic Zones, Lampung Block Seismotectonic Zone and Center Part of Sunda Strait Seismotectonic Zone. Based on these seismic source zones, the Probabilistic Seismic Hazard Analyses (PSHA) of Sunda Strait have maximum Peak Ground Acceleration (PGA)=0.465g, Pseudo Seismic Acceleration (PSA) Ss=0.2 second=1.114 g, PSA S1=1second=0.465g in Site Class SB at 7% probability in 75 years (equivalent to a mean return of 1000 years), maximum Peak Ground Acceleration (PGA)=0.484g, Pseudo Seismic Acceleration (PSA) Ss=0.2 second=1.159 g, PSA S1=1second=0.484g in Site Class SB at 2% probability in 50 years (equivalent to a mean return of 2500 years), Peak Ground Acceleration (PGA)=0.499g, Pseudo Seismic Acceleration (PSA) Ss=0.2 second=1.193g, PSA S1=1second=0.499g, in Site Class SB at 2% probability in 100 years (equivalent to a mean return of 5000 years). The results of this effort are expected to be used as the primary data for seismic risk assessment in the Sunda Strait and its surrounding area.

20

Keywords: seismotectonic, PSHA, Sunda strait, seismic source zones

1 Introduction

The Sunda Strait is one of the earthquake-prone regions in western Indonesia. This strait is the gateway connecting the mainland of Sumatra and Java islands. The growth of strategic industries in this area is accompanied by population growth and the rapid development of residential areas, services, and tourism. It is considering the density of land used in the land region and its coastal zone, which are vulnerable to seismic risk. Therefore, a seismotectonic study and seismic hazard assessment have been conducted to prevent the effects of seismic risks. The seismotectonic in Sunda Strait can be interpreted as a transition zone between the oblique asymmetric subduction zone in western Sumatra and the frontal asymmetric subduction zone in southern Java (Huchon and Pichon, 1984; Harjono et al., 1991).

25



30 Furthermore, this area's seismicity could be used as data and information about present geotectonic activities, Pramumijoyo and Sebrier, 1991. It will concisely illustrate the relationship between tectonics and the occurrence of earthquakes in particular regions. It presents basic information regarding the tectonic setting, the late tectonic activities, and seismicity. Nevertheless, this data does not automatically explain the seismic risk, but it only provides essential information for evaluating seismogenic sources and potential seismic hazards to mitigate the seismic risk. The seismotectonic is also used to examine many strategies, such as those conducted by Adinolfi et al., 2021; Rakshit et al., 2022, and their parameters and zones (Razaghian et al., 2018; Ahadov and Ozturk, 2021; Mammadli, 2022; Omishi et al., 2022). In order to create a seismic hazards map in the Sunda Strait region, a probabilistic seismic hazard assessment (PSHA) will be applied to the seismic hazard zonation map. Even though the controversy of the PSHA analysis is still debatable (Stein et al., 2011), this method is still used worldwide (e.g., Shedlock et al., 2000; Kowsari et al., 2022; Ordaz et al., 2022). Thus, this study aims to reveal the updated seismotectonic situation in Sunda Strait as a new insight due to the risk of seismic hazards by using PSHA as a basis for zonation.

2. Data and Methods

The geological data has been used from the systematic geological map on a scale of 1: 100.000 (Java) and 1:250.000 (Sumatera) published by the Center of Geological Survey, Amin et al., 1993; Andi et al., 1993. The seismicity and focal mechanism have been applied for the coordinate of 103° East to 107° East and 4° South to 10°30' South from the Global Centroid Moment Tensor (GCMT), the United States Geological Survey Earthquake Catalog and International Seismological Center Earthquake Catalog. The seismicity of this region was collected from PDE USGS Earthquake and Global Centroid Moment Tensor Catalogs at coordinates of -10.51° to -4.071° and 103.001° to 107°. Duration of the earthquakes catalogue is 1976 until 2022, range of magnitude $4.4 \leq M_w \leq 6.9$ (309 records), $3.4 \leq M_b \leq 5.9$ (1939 records), and $4.9 \leq M_s \leq 6.3$ (17 records), range of depth 3.6 to 640.8 km.

50 The research methodology started with evaluating and analyzing geological and seismicity parameters. It included an assessment of the stratigraphy and lithology, structural geology, seismicity, and focal mechanism. The earthquakes Magnitude Distribution for each zone attempts to determine the yearly seismicity rate for each location. Earthquakes of varying magnitudes may be caused by tectonic faults (i.e., magnitudes). The previous study analyzed the observations of earthquake magnitudes and discovered that the distribution of these earthquake sizes in an area follows a specific distribution, as shown by Zuniga et al., 2020; Beydokhti and Abbaspour (2015), which calculated based on Gutenberg and Richter (1954) as a pioneer in this design. The distribution of these earthquake sizes in a region generally follows a particular distribution, given as follows.

$$\log(N) = a - bm \quad (2.1)$$

N is the earthquakes rate with magnitudes greater than m, and a and b are constants. This equation is called the Gutenberg-Richter recurrence law. The model of this distribution is one of seismic activity within the area. The a and b values, as one key parameter of PSHA, can be used to characterize the area. The a and b constants from equation (2.1) are estimated using



statistical analysis of historical observations in each zonation, with additional constraining data provided by other types of geological evidence. The a value indicates the overall rate of earthquakes in a region, and the b value indicates the relative ratio of small and large magnitudes.

Since the seismotectonic and seismic source zone analyses are used as the primary data for PSHA, thus, they have been determined in each seismic source zone. The Probability Density Function (PDF) for magnitude M for this seismicity area with minimum magnitude $m_{\min} = 4.1$ and maximum magnitude $m_{\max} = 6.5$, and probabilities of occurrence for the discrete set of magnitudes 4 to 7 can be found as follow:

$$\begin{aligned} F_M(m) &= P(M \leq m | M > m_{\min}) \\ &= \frac{\text{Rate of Earthquake with } m_{\min} < M \leq m}{\text{Rate of Earthquake with } m_{\min} < M} \\ 70 \quad &= \frac{\lambda m_{\min} - \lambda m}{\lambda m_{\min}}, m > m_{\min} \end{aligned} \quad (2.2)$$

$F_M(m)$ is the Cumulative Distribution Function for M . computation of the Probability Density Function (PDF) for M by taking the PDF derivative.

$$PDF(m) = \frac{d}{dm} F_M(m), m > m_{\min} \quad (2.3)$$

The probabilities of occurrence of these discrete sets of magnitudes, assuming that they are the only possible magnitudes, and computed as follows

$$P(M = m_j) = F_M(m_{j+1}) - F_M(m_j) \quad (2.4)$$

Where m_j are the discrete set of magnitudes, ordered so that $m_j < m_{j+1}$, this calculation assigns the probabilities associated with all magnitudes between m_j and m_{j+1} to the discrete m_j , the approximation will not affect numerical results as long as the discrete magnitudes are closely spaced.

80 The GMPEs model reflects the model of the propagation of earthquake waves from an earthquake source location for each type of earthquake to location observations which are expressed by mathematical models that are very specific for each region. Ideally, the local attenuation equation calculates earthquake hazards in an area study. Still, due to the unavailability of an empirical equation model for the Indonesian region, the PSHA process in this study selected several empirical equations obtained from the place of others. GMPE selection uses the OpenQuake software, Weatherill, 2015 and Pagani et al., 2014 for
85 processing computational earthquake hazard assessment. Several GMPE models are used in this study and refer to the models commonly used in some references, namely to the source of the earthquake megathrust, Zhao et al., 2006 and the source of the earthquake fault (shallow crustal): Boore et al., 2014; Campbell et al., 2014; Chiou and Youngs, 2014.

Ground Motion Prediction Equations (GMPEs) used to estimate ground motions in this study are the Chiou and Youngs, 2014. GMPEs provide a means of predicting the level of ground shaking and its associated uncertainty at any given site or location



90 based on an earthquake magnitude, source-to-site distance, local soil conditions, and fault mechanisms. The documentation and programs for these NGA WEST-2 GMPEs 2014 were downloaded from the PEER website.

Site class is any site with bedrock underneath approximately 3 m of the ground surface. Five zones of interest are laid on the surface with average seismicity Velocity Shear 30 meters deep (V_{s30}) according to the BSN,SNI-1726-2019 shown in Table 1.

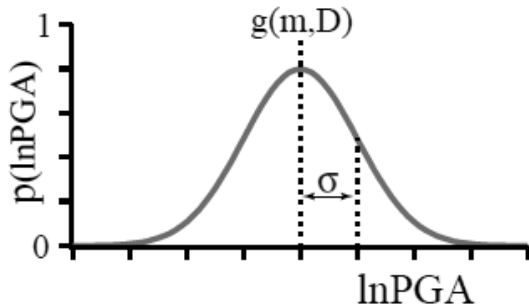
95

Table 1: Site Class V_{s30} (BSN, SNI 1726:2019)

Site Class	V_s (m/sec)	N or N_{ch}	S_u (kPa)
SA (hard rock)	>1500	N/A	N/A
SB (rock)	750 until 1500	N/A	N/A
SC (hard soil, very congested and soft rock)	350 until 750	>50	≥ 100
SD (moderate soil)	175 until 350	15 until 50	50 until 100

100 The seismic-hazard source model has provided N earthquake scenarios E_n , which has an associated magnitude (m_n), location (L_n), and rate (r_n). The scenario of location can determine the distance D_n to the site. Based on m_n and D_n , the attenuation relationship shows that the distribution of possible ground-motion levels for this scenario is (figure 1):

$$P_n(\ln PGA) = \frac{1}{\sigma_n \sqrt{2\pi}} e^{-(\ln PGA - g(m_n, D_n))^2 / 2\sigma_n^2} \quad (2.5)$$



105 **Figure 1. lnPGA and Standard deviation**

Where $g(M_n, D_n)$ and σ_n are the mean and standard deviation of $\ln PGA$ given by the attenuation relationship, the integration of $P_n(\ln PGA)$ is known as the probability exceeding each $\ln PGA$ (figure 2).

$$P_n(\ln PGA) = \int_{\ln PGA}^{\infty} \frac{1}{\sigma_n \sqrt{2\pi}} e^{-(\ln PGA - g(m_n, D_n))^2 / 2\sigma_n^2} d\ln PGA \quad (2.6)$$

110

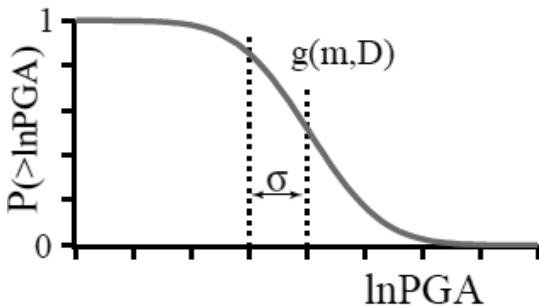


Figure 2. Probability PGA Occurance

It gives the probability of exceeding each lnPGA where the event is to occur. If we multiply this by r_n , we get the annual rate at which each lnPGA is exceeded (R_n) due to the scenario:

$$115 \quad R_n (> \ln \text{PGA}) = r_n P_n (> \ln \text{PGA}) \quad (2.7)$$

This sum of overall N scenarios, we get the total annual rate of exceeding each lnPGA:

$$R_{\text{tot}} (> \ln \text{PGA}) = \sum_{n=1}^N R_n (> \ln \text{PGA}) = \sum_{n=1}^N r_n P_n (> \ln \text{PGA}) \quad (2.8)$$

Using the Poissonian distribution, the compute the probability of exceeding each Ground-motion level in the following T years from this annual rate as:

$$120 \quad P_{\text{pois}} (> \ln \text{PGA}, T) = 1 - e^{-R_{\text{tot}} T} \quad (2.9)$$

3. Result and Discussion

3.1 Geology and Tectonic of Sunda Strait

The geology of the inland region of Sunda Strait and its surroundings has been compiled from geological maps of the Sumatra region at a scale of 1: 250.000 on the Tanjungkarang sheet (Andi et al., 1993) and Liwa sheet (Amin et al., 1993) and geological maps Java region at a scale of 1: 100.000 are Anyer sheet (Santosa, 1991) and Cikarang sheet (Sudana and Santosa, 1992). Especially for the oceanic region, the structural geology has been re-linearized and simplified from Susilohadi et al., 2009. Based on this map, the geology of Sunda Strait and the surrounding area can be divided into the oldest Mesozoic Metamorphics Group and the Cretaceous Intrusives Group in the southern part of Sumatera Island. Unconformable in these oldest groups found the Transitional Sediments Group. The oldest Mesozoic Group and Cretaceous Intrusives Group on Java Island are not located. The oldest group is the Paleosen-Oligosen of Transitional Sediments Group in western Java. Unconformable on the Paleosen-Oligosen Transitional Sediments Group, the Marine Sediments Group was intruded by Middle Miocene Intrusives Group. Unconformable on this Marine Sediments Group overlain the Volcanic Group. In several western Java and southern Sumatra locations, this volcanic group intruded by the Pliocene-Pleistocene Intrusives Group. The Volcanics of Krakatau



Group was the youngest volcanic product in this region. Several sites of this region, especially the lowland area and the coastal zone, are covered by the Surface Sediments Group, consisting of alluvium and terrace.

The Sunda Strait lies between Sumatra Island's oblique asymmetry subduction and Java's frontal asymmetry subduction. These different tectonic conditions make the Sunda Strait an extension tectonic region. The emergence of young and old volcanoes in the Sunda Strait and the mainland of Lampung is controlled by extensions tectonic system, such as Panaitan Tua Volcano, Anak Krakatau Active Volcano, Sebesi Old Volcano - Sebuku, Rajabasa, and Sukadana Old Volcanoes as a feature of the Sunda Strait. This region's earthquake and tsunami hazard originates from the active tectonic zones and active volcanoes. This region's active tectonic source zones are of subduction between India's active oceanic tectonic plate - the Australian and the active continental tectonic plates of the Eurasian. Besides, active seismotectonic source zones are also triggered by Sumatera Fault, Lampung Fault, Panaitan - Krakatau – Rajabasa Fault, and Banten Fault. Based on the geological and tectonic conditions, this area has four tectonic periods: Paleogene, Oligo-Miocene, Plio-Pleistocene, and Holocene. Figure 3 depicts the Sunda Strait and its surroundings' stratigraphy, lithology, and tectonic era. The unconformable tectonic stratigraphy shows every tectonic period in this region. Based on stratigraphy and lithology, this area can be classified into two majors. The bedrock consists of metamorphic/Pre-Tertiary and marine sediments/Tertiary. The near-surface rock consists of volcanic rock and alluvium/Quaternary. The contrast of the physical properties of these two lithological groups is an index of the potential for seismic hazard in this region.

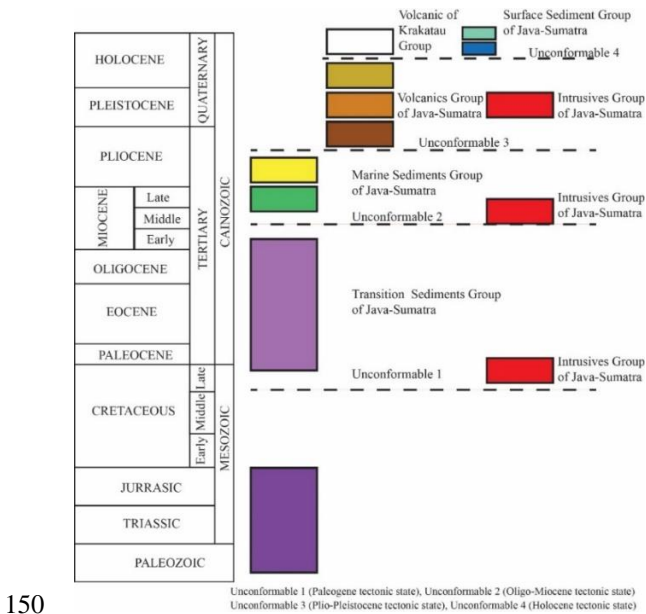


Figure 3. Tectono Stratigraphy of Sunda Strait and Surrounding area.

3.2 Seismicity of Sunda Strait

The distribution analysis is based on the earthquake epicenter's focal depth and focal mechanism. The results demonstrated that subduction tectonic activities between the Indian-Australian oceanic plate and the Eurasian continental tectonic plates



155 cause the most frequent earthquakes. Active fault seismic sources follow this incident in and near the Sunda Strait, including the Sumatra active fault (SAF), Mentawai active fault, Lampung active fault, and Banten-Ujungkulon active fault, as can be seen in figure 4.

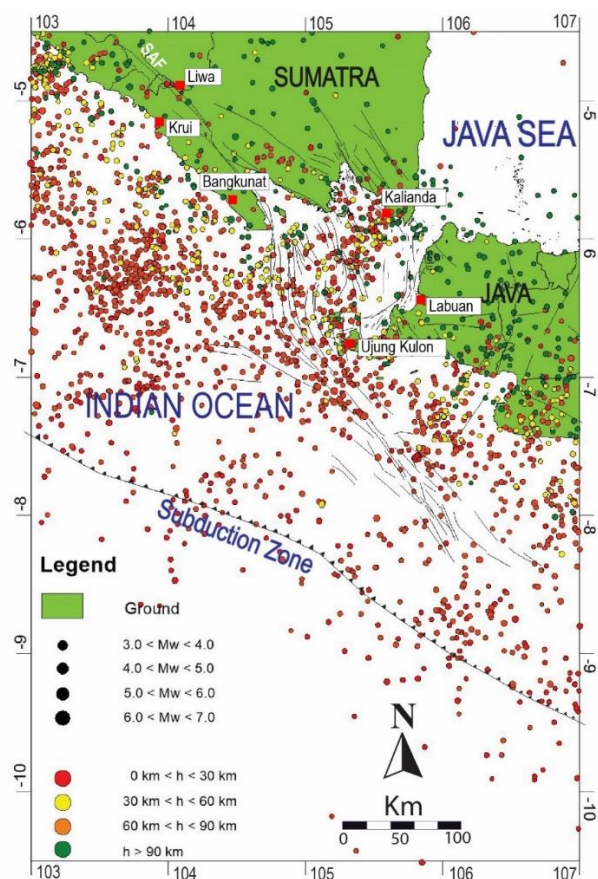


Figure 4. Seismicity map of Sunda Strait and surrounding area, modified from USGS, 2022

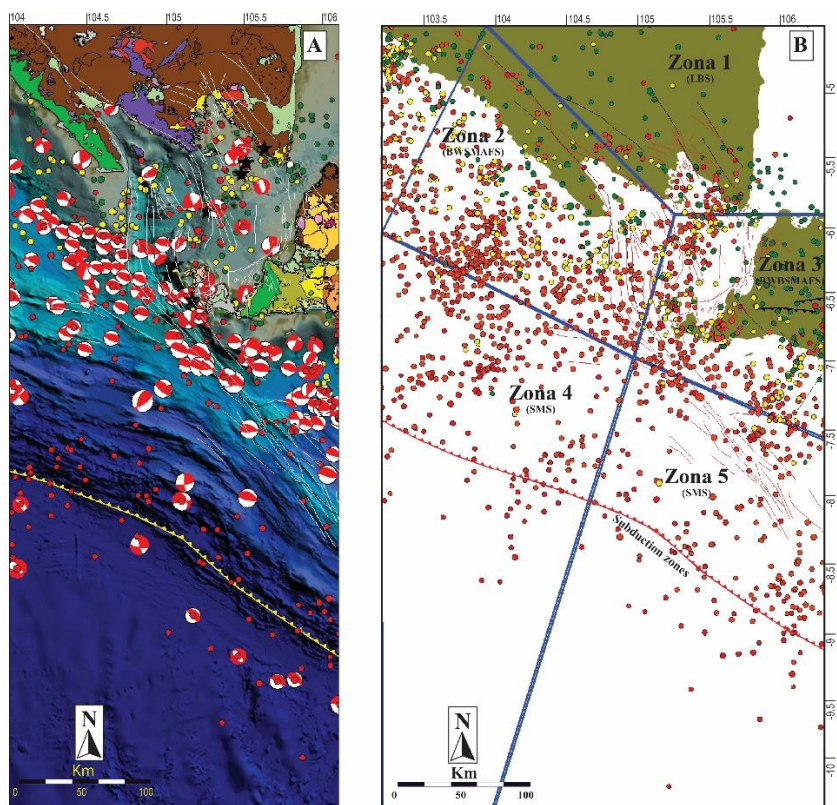
160 3.4 Seismotectonic and Seismic Source Zones of Sunda Strait

The seismotectonic analysis is extensively used in numerous regions of the globe, such as Imaeva et al., 2018 in Siberia, Mulabisana et al., 2021 in Azerbaijan, and Rakhsit et al., 2022 in northeast India. According to the earthquake's magnitude distribution, the Sunda Strait and surrounding area have three seismotectonic provinces: the Asymmetry Oblique Subduction Seismotectonic Province of western Sumatra Island, the Asymmetry Frontal Subduction Seismotectonic Province of southern Java Island, and the Asymmetry Extension Seismotectonic Province of Sunda Strait. Generally, this region's earthquakes are associated with the Asymmetry Oblique Subduction Seismotectonic Province and show the focal mechanism of the thrust fault mechanism. Similar earthquake focal mechanisms are related to the Asymmetry of Frontal Subduction Seismotectonic Province. In contrast to the earthquakes associated with the Asymmetry Extension, Seismotectonic Province show the strike-slip fault and normal fault focal mechanisms. Based on these parameters, the seismotectonic zones around Sunda Strait may



170 be classified into five (5) zones, Sunda Megathrust Seismotectonic/SMS Zones (Z4 and Z5), Benioff Wadati Sumatra and
Mentawai Active Faults Seismotectonic Zone/BWSMAFS (Z2), Benioff Wadati and Banten Active Faults Seismotectonic
Zone/BWBAFS (Z3) and Lampung Block Seismotectonic Zone/LBS (Z1).

The seismotectonic map and seismotectonic zones as the seismic source zone of Sunda Strait and surrounding areas are shown
in Figure 5A-B. These seismotectonic provinces have been used as seismic sources in probabilistic seismic hazard studies.



175

Figure 5. Seismotectonic map and Seismic Source Zone of Sunda Strait

The a and b constants from equation (2.1) are estimated using statistical analysis of historical observations in each zonation, with additional constraining data provided by other types of geological evidence. The a value indicates the overall rate of earthquakes in a region, and the b value indicates the relative ratio of small and large magnitudes, Figure 6.

180

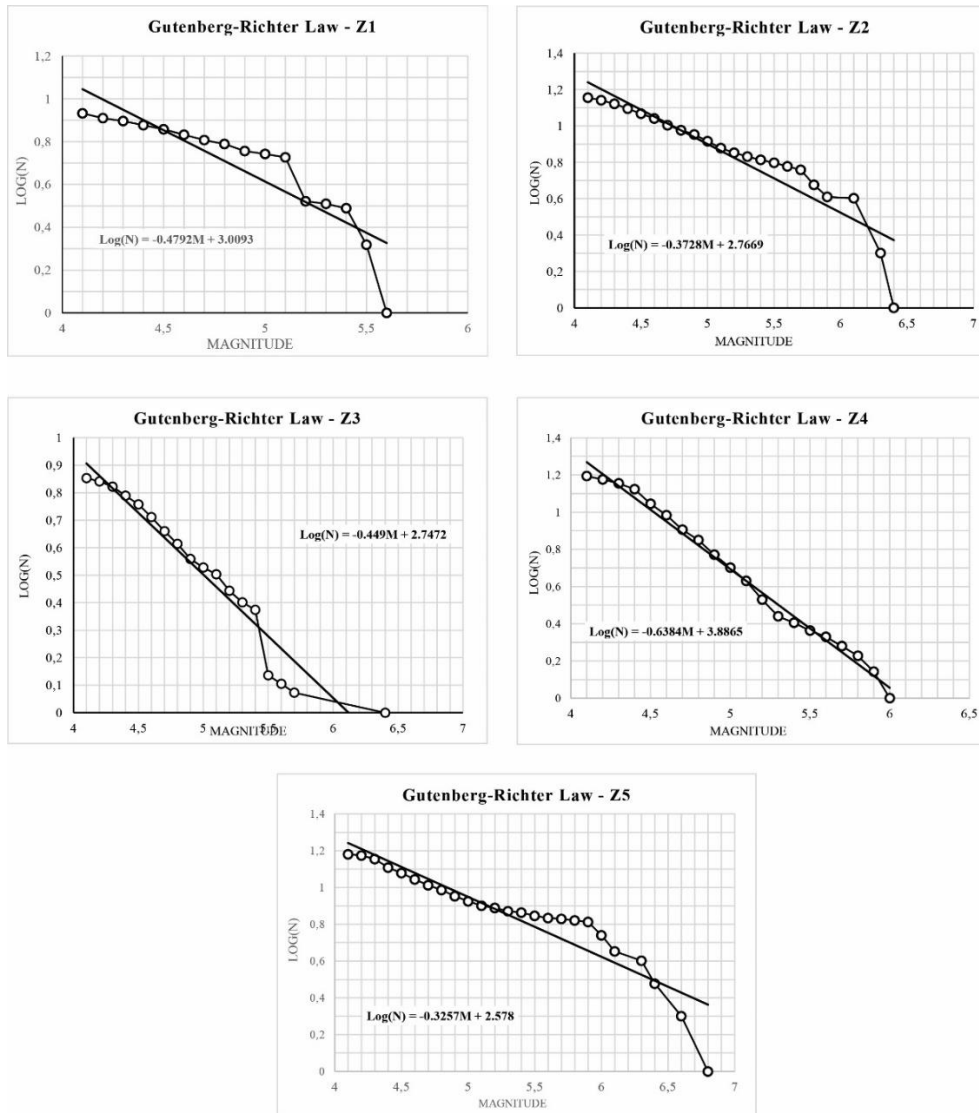


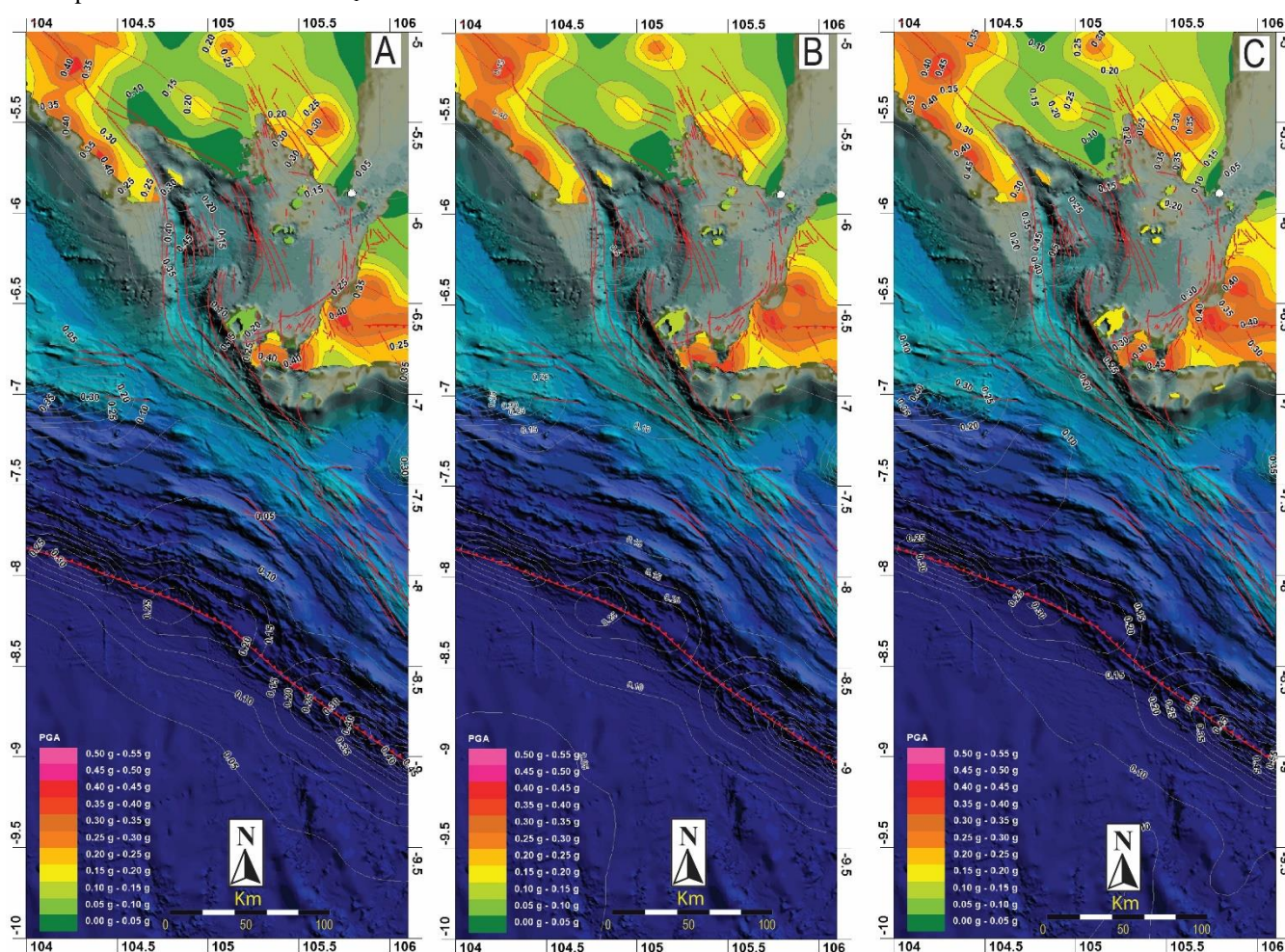
Figure 6. Guttenberg and Richter function for the zones of the Sunda Strait region

3.5 Probabilistic Seismic Hazard Analyses (PSHA)

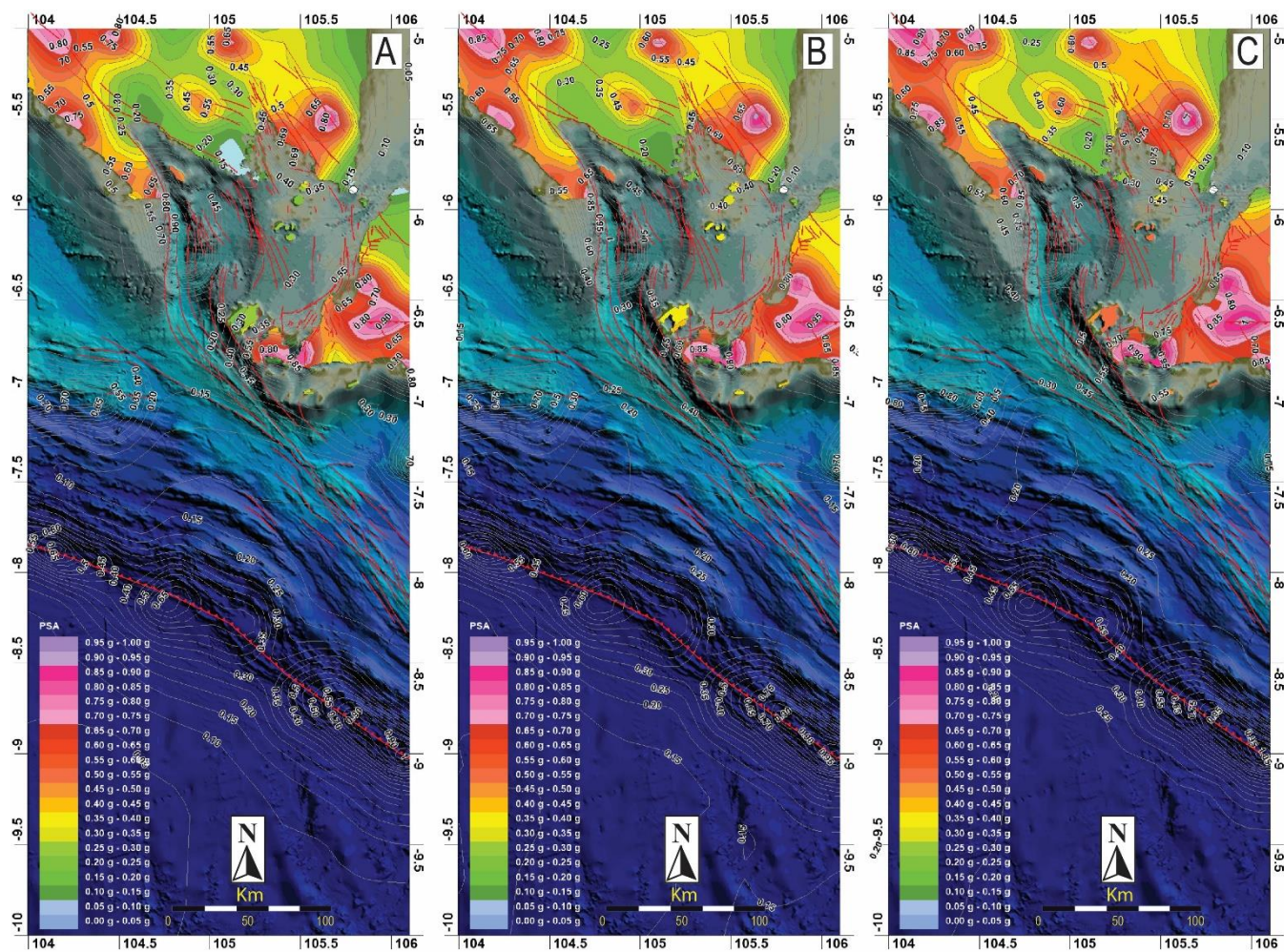
185 Probabilistic Seismic Hazard Analyses of this region have been completed to produce the PGA (figure 7) and PSA maps. The PSA consists of PSA short period $S_s=0,2$ second and PSA long period $S_l= 1$ second, shown in figures 8 and 9. Based on these maps, in general, the inland region of Sunda Strait can be divided into regions of $\text{PGA} < 0.20g$, $\text{PGA} > 0.20g-0.35g$, and $\text{PGA} > 0.35-0.40g$ and for PSA $S_s=0.2$ second divided into regions of $\text{PSA} < 0.30 g$, $\text{PSA} > 0.30-0.40g$, $\text{PSA} > 0.40-0.55g$ and $\text{PSA} > 0.55-0.90g$. PSA $S_l=1$ second divided into regions of $\text{PSA} < 0.20g$, $\text{PSA} > 0.20-0.40g$, and $\text{PSA} > 0.40g$. Probabilistic Seismic Hazard Analyses (PSHA) of Sunda Strait have maximum Peak Ground Acceleration (PGA)=0.465g, Pseudo Seismic



190 Acceleration (PSA) $S_s=0.2$ second=1.114 g, PSA $S_1=1$ second=0.465g in Site Class SB at 7% probability in 75 years (equivalent to a mean return of 1000 years), maximum Peak Ground Acceleration (PGA)=0.484g, Pseudo Seismic Acceleration (PSA) $S_s=0.2$ second=1.159 g, PSA $S_1=1$ second=0.484g in Site Class SB at 2% probability in 50 years (equivalent to a mean return of 2500 years), Peak Ground Acceleration (PGA)=0.499g, Pseudo Seismic Acceleration (PSA) $S_s=0.2$ second=1.193g, PSA $S_1=1$ second=0.499g, in Site Class SB at 2% probability in 100 years (equivalent to a mean return of 5000 years). The
 195 PGA and PSA map shows the high PGA, and PSA concentrated in the Liwa, Krui until Bangkunat, Kalinda (Sumatera), Ujungkulon, and Labuan (Java). Comparison of the maximum acceleration value of PSHA of 1000, 2500, and 5000 years return period for PGA and PSA $S_1=1$ second is 2% and for PSA $S_s=0.2$ second is 4%.

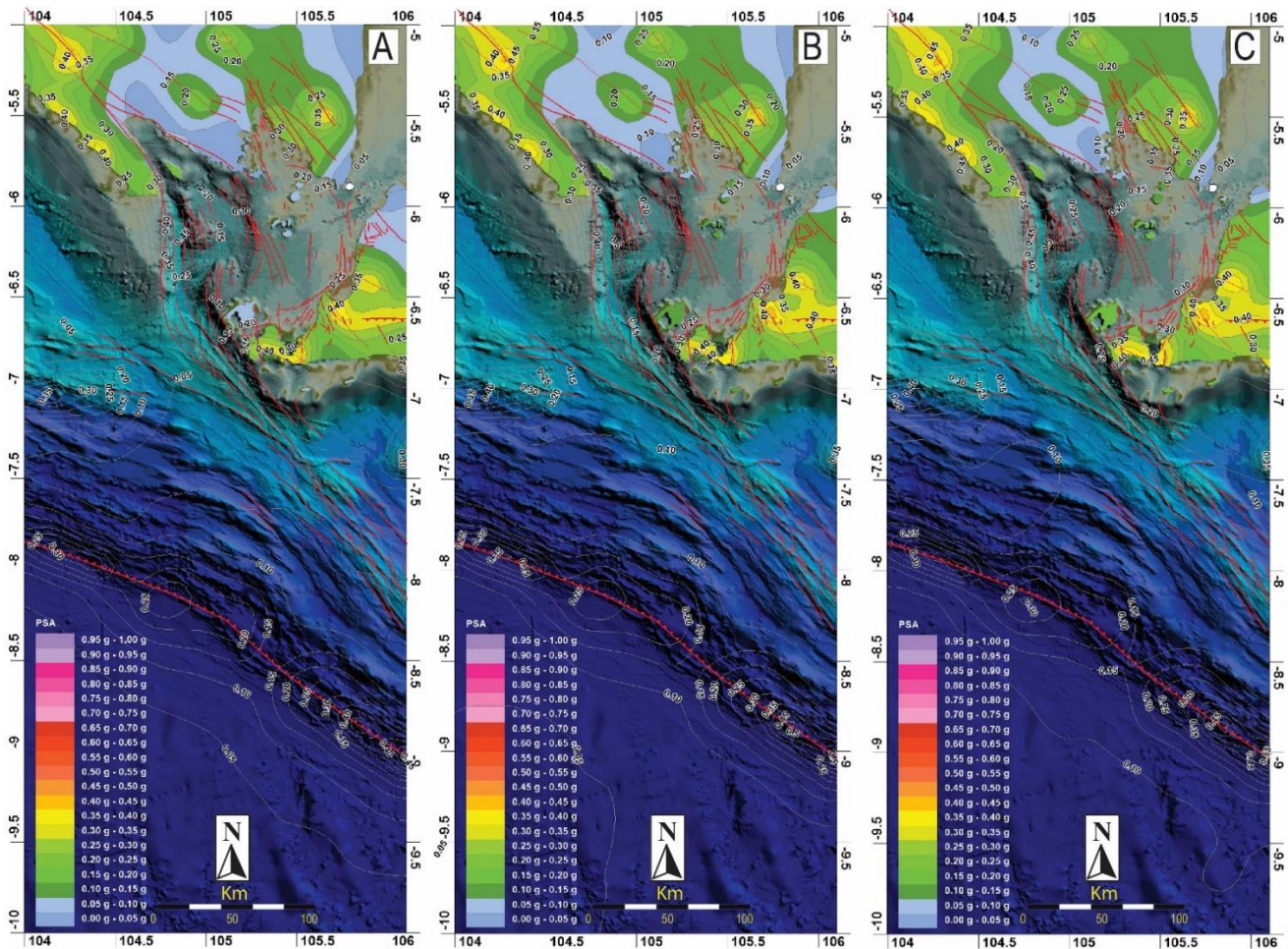


200 **Figure 7. Sunda Strait seismic hazard reference map, displaying the mean value of peak ground acceleration (PGA): figure A with a 2% probability of being surpassed in 50 years (equivalent to a mean return of 2500 years) assessed for a rock soil (VS 30 = 750-1500 m/s); figure B: with a 7% probability of being surpassed in 75 years (equivalent to a mean return of 1000 years) assessed for a rock soil (VS 30 = 750-1500 m/s); figure C: with a 2% probability of being surpassed in 100 years (equivalent to a mean return of 5000 years) assessed for a rock soil (VS 30 = 750-1500 m/s).**



205

Figure 8. Sunda Strait, seismic hazard reference map, displaying the mean value of probabilistic seismic hazard analysis (PSHA): figure A shows a 7.5% damped with $T=0.2$ second 2% probability of being surpassed in 50 years, figure B shows a 5% damped with $T=0.2$ second 7% probability of being surpassed in 75 years; and figure C shows a 5% damped with $T=0.2$ second 2% probability of being surpassed in 100 years.



210

Figure 9. Sunda Strait, seismic hazard reference map, displaying the mean value of probabilistic seismic hazard analysis (PSHA): figure A shows a 7.5% damped with $T=1$ second 2% probability of being surpassed in 50 years, figure B shows a 5% damped with $T=1$ second 7% probability of being surpassed in 75 years, and figure C shows a 5% damped with $T=1$ second 2% probability of being surpassed in 100 years.

215

According to the Indonesian Standardization Agency, the PSHA of 2% probability of being surpassed in 50 years at site class SB is used as the primary data to assess potential seismic hazard and risk for building and non-building (BSN, SNI 1726:2019), the PSHA of 7% probability of being surpassed in 75 years at site class SB on assess potential seismic hazard and risk for a bridge (BSN, SNI 2833:2016) and 2% probability of being surpassed in 100 years at site class SB on assess potential hazard and risk for analysis of the stability of the static slopes of the dam (BSN, SNI 8064:2016).

220

4 Conclusions

This study provided new insight into the seismotectonic circumstances in the Sunda Strait region by updating the zoning seismic source zone around the Sunda strait and demonstrating the probabilistic seismic hazard analysis (PSHA). The Active



Subduction Zone of the Sunda Arc and shallow crust active faults are the primary potential seismic source that controls the potential seismic hazard of this region. High PGA and PSA index inland regions are concentrated in Liwa, Krui until
225 Bangkunt, Kalinda (Sumatera), Ujungkulon, and Labuan (Java). The maximum PGA is 0.465g, 0.484, and 0.499, PSA $S_s=0.2$ seconds are 1.114g, 1.159g, and 1.193g, and PSA $S_1=1$ second are 0.465g, 0.484g and 0.499g (return period of 1000, 2500 and 5000 years). According to BSN SNI, these potential seismic hazard indexes are expected to assess this region's potential seismic risk in implementing infrastructure development regulations.

Author contribution

230 All the authors compiled, validated and analysed data used in this work. Conceptualization: AS, FN, and MR; methodology: AS, FN, MR; software analysis: AS and FN, MR.; manuscript preparation: AS, FN, MR, MCF, and S.; review and editing: AS and FN; figures: AS and FN.

Competing interest

The contact author has declared that none of the authors has any competing interests.

235 Acknowledgments

The authors thank our National Research and Innovation Agency (BRIN) and Seismotectonic Working Group colleagues in the Centre for Geological Survey, Geological Agency, Ministry of Energy, and the Mineral Resources Republic of Indonesia for supporting to completion of this scientific article.

References

- 240 Adinolfi, G.M., De Matteis, R., de Nardies, R., and Zollo, A.: A functional tool to explore the reliability of micro-earthquake focal mechanism solutions for seismotectonic purposes., *Solid Earth*, 13, 65-83, doi:10.5194/se-13-65-2022, 2022.
- Ahadov, B and Ozturk, S.: Spatial variations of fundamental seismotectonic parameters for the earthquake occurrences in the Eastern Mediterranean and Caucas. *Natural Hazards*, 10.1007/s11069-021-05170-1, 2021.
- Amin, T.C., Sidarto., Santosa, S and Gunawan, W.: Geological map of Kotaagung quadrangle, Sumatera, the scale of 1:250.000,
245 Geological Research and Development Centre, Bandung, 1993.
- Andi, S, M., Amirudin., Suwarti, T., Gafoer, S and Sidarto.: Geological map of Tanjungkarang quadrangle, Sumatera, the scale of 1:250.000, Geological Research and Development Centre, Bandung, 1993.
- BSN, SNI 1726:2019.: Tata cara perencanaan ketahanan gempa untuk struktur bangunan gedung dan non gedung, Badan Standarisasi Nasional (BSN), Indonesia, 238p, 2019.



- 250 BSN, SNI 2833:2016.: Perencanaan jembatan terhadap beban gempa, Badan Standarisasi Nasional (BSN), Indonesia, 60p, 2016.
- BSN, SNI 8064:2016.: Metode analisis stabilitas lereng statis bendungan tipe urugan, Badan Standarisasi Nasional (BSN), Indonesia, 28p, 2016.
- Beydokhti, M. K., and Abbaspour, R. A.: Determination of the Number of Seismotectonic Provinces using Partitioning Cluster of Seismic Data, *Journal of Geospatial Information Technology*, 3, 1, 1-13, 2015.
- 255 Boore, D. M., Stewart, J. P., Seyhan, E., Atkinson, G. M.: NGA-West2 equations for predicting PGA, PGV, and 5% damped PGA for shallow crustal earthquakes, *Earthq. Spectra* 30, 3, 1057–1085, 2014.
- Campbell, K. W., and Bozorgnia, Y.: NGA-West2 Campbell-Bozorgnia ground motion model for the horizontal components of PGA, PGV, and 5%-damped elastic pseudo-acceleration response spectra for periods ranging from 0.01 to 10 sec, *Earthq. Spectra* 30, 1087–1115, 2014.
- 260 Chiou, B, S, J., and Youngs, R, R., MERRI.: Update of the Ground Motion Model for Average Horizontal Component of Peak Ground Motion and Response Spectra, *Earthquake Spectra* 30, 3, 1117-1153, doi:10.1193/072813EQS219M, 2014.
- Chiou, B, S, J., and Youngs, R: Update of the Chiou and Youngs NGA model for the average horizontal component of peak ground motion and response spectra, *Earthq. Spectra* 30, no. 3, 1117–1153, doi: 10.1193/072813EQS219M, 2014.
- 265 Global Centroid Moment Tensor (Catalog Search: <https://www.globalcmt.org/CMTsearch.html>, last access 02 February 2022.
- Gutenberg, B., Richter, C.F.: *Seismicity of the Earth and Associated Phenimena*. Princeton University Press Princeton, New Jersey, pp. 310, 1954.
- Harjono, H., Diament, M., Dubois, J., Larue, M. and Zen, M.T. Seismicity of the Sunda Strait: Evidence for Crustal Extension and Volcanological Implications. *Tectonics*, 10, 1, 17-30. 10.1029/90TC00285. 1991.
- 270 Huchon, P. dan Le Pichon. Sunda Strait and Central Sumatera Fault. *Geology*, 12, 668-672, doi:10.1130/0091-7613(1984)12<668:SSACSF>2.0.CO;2, 1984.
- Imaeva, L. P., Imaev, V.S., Koz'min, B. M.: Seismotectonic Activation of Modern Structures of the Siberian Craton. *Geotectonics*, 52, 6, 618-633, doi: 10.1134/S0016852118060031, 2018.
- International Seismological Centre Bulletin: <http://www.isc.ac.uk/iscbulletin/search/fmechanisms/interactive/>, last access 02
- 275 February 2022.
- Kowsari, M., Ghasemi, S., Bayat, F., Halldorsson, B.: A Backbone Seismic Ground for Strike-slip Earthquakes in Southwest Iceland and its Implications for Near-And Far-field PSHA. *Bulletin of Earthquake Engineering*. 9, 4, 931-953, doi:10.21203/rs.3.rs-1689834/v1, 2022.
- Mammadli, T. Ya.: Determination of Seismogenic Zones for Analysis of Seismotectonic Activity of Deep Faults: Seismic Hazard Assessment for the Territory of Azerbaijan. *Geotectonics*, 56, 2, 191-199, doi: 10.1134/S0016852122020042, 2022.
- 280 Mulabisana, T., Meghraoui, M., Midzi, V., Saleh, M., Nitibinyanes, O., Kwadiba, T., Manzuzu, B., Siphemo, O., Pule, T., Saunders.: Seismotectonic analysis of the 2017 moyiabana earthquake (Mw 6.5; Botswana), insight from field



- investigations, aftershock, and InSAR studies. *Journal of African Earth Sciences*, 182, 104297, doi:10.1016/j.jafrearsci.2021.104297, 2021.
- 285 Omishi, K., Kumamoto, T., Mori, K. Advanced and More Objective Model of Seismotectonic Province Map in the Japanese Islands, Employing Multivariate Analysis. *Journal of Japan Association for Earthquake Engineering*. 22, 1, 1-15. Doi:10.5610/jaee.22.1_1, 2022.
- Ordaz, M., Manica, M.A., Salgado-Salvez, M. A., Osorio, L.: Inclusion of site-effects: an approach coherent with contemporary event-based PSHA practices. *Soil Dynamics and Earthquake Engineering*, 158, 107286, doi:10.1016/j.soildyn.2022.107286, 2022.
- 290 Pacific Earthquake Engineering Research Center (PEER): https://peer.berkeley.edu/ngawest/nga_models.html, last access 14 February 2022.
- Pramumijoyo, S and Sebrier, M.: Neogen and Quaternary fault kinematics around the Sunda Strait area, Indonesia. *Journal of Southeast Asian Earth Sciences*, 6, 2, 137-145, 1991.
- 295 Rakhsit, R., Bezbaruah, D., Zaman, F., Bharali, B., Saika, S.: Locked crustal faults associated with the subducting Indian Lithosphere and its implications in seismotectonic activity in the Central Indo-Burmese Ranges, Northeast India. *Geofizika*, 39, 5, 163-178. doi:10.15233/gfz.2022.39.5, 2022.
- Razaghian, G., Beitollahi, A., Pourkermani, M., Arian, M. Determining seismotectonic provinces based in seismicity coefficients in Iran. *Journal of Geodynamics*, 119, 29-46, doi: 10.1016/j.jog.2018.05.007, 2018.
- 300 Santosa, S.: Geological map of Anyer quadrangale, Java, scale of 1:250.000, Geological Research and Development Centre, Bandung, 1991.
- Sudana, D and Santosa, S., 1992. Geological map of Anyer, Java, the scale of 1:250.000, Geological Research and Development Centre, Publish.
- 305 Stein, S., Geller, R., & Liu, M.: Bad assumptions or bad luck: Why earthquake hazard maps need objective testing. *Seismological Research Letters*, 82, 5, 623–626. doi:10.1785/gssrl.82.5.623, 2011.
- Susilohadi. S., Gaedicke, C., Djajadihardja., Y.: Structures and sedimentary deposition in Sunda Strait, Indonesia. *Tectonophysics*, 467, 1-4, 55-71. doi:10.1016/j.tecto.2008.12.015, 2009.
- United States Geological Survey (USGS) Earthquake Catalog: <https://earthquake.usgs.gov/earthquakes/search/>, last access 14 March 2022.
- 310 Weatherill, G.: OpenQuake ground motion toolkit-User guide, Global Earthquake Model (GEM), Technical Report, 2015.
- Zhao, J. X., K. Irikura, J. Zhang, Y. Fukushima, P. G. Somerville, A. Asano, Y. Ohno, T. Oouchi, T. Takahashi, and H. Ogawa.: An empirical site-classification method for strong-motion stations in Japan using H/V response spectral ratio, *Bull. Seismol. Soc. Am.* 96, 3, 914–925, 2006..
- 315 Zuniga F, R., Lacan, P., Rodriguez-Perez, Q, Marquez-Ramirez, V, H.: Temporal and spatial evolution of instrumented seismicity in the Trans-Mexican Volcanic Belt. *J S Am Earth Sci*, 98, 102390, doi: 10. 1016/j. jsames. 2019. 102390, 2020.